Electromagnetically induced grating with maximal atomic coherence

Silvânia A. Carvalho and Luís E. E. de Araujo*

Instituto de Física "Gleb Wataghin," Universidade Estadual de Campinas, Campinas-SP, 13083-859 São Paulo, Brazil

(Received 27 June 2011; published 31 October 2011)

We describe theoretically an atomic diffraction grating that combines an electromagnetically induced grating with a coherence grating in a double-Λ atomic system. With the atom in a condition of maximal coherence between its lower levels, the combined gratings simultaneously diffract both the incident probe beam as well as the signal beam generated through four-wave mixing. A special feature of the atomic grating is that it will diffract any beam resonantly tuned to any excited state of the atom accessible by a dipole transition from its ground state.

DOI: 10.1103/PhysRevA.84.043850 PACS number(s): 42.50.Gy, 42.65.−k

I. INTRODUCTION

Electromagnetically induced transparency (EIT) [1] allows a diffraction grating to be induced in an atomic sample. Electromagnetically induced gratings (EIGs) have been applied to all-optical switching and routing [2], tunable photonic band gaps [3], light storage [4,5], and beam splitting and fanning [6], among other applications. The physical basis of EIT is coherent population trapping (CPT) [7], which decouples the atom from the excitation fields by placing it into a nonabsorbing, dark superposition state of the atom's lower energy levels. EIT of a resonant probe beam is achieved in a three-level atom by means of a coupling field acting on a linked transition. In an atom under EIT, an EIG can be created by modulating the atomic absorption or dispersion. An absorption EIG is implemented by spatially modulating the coupling field (for example, by superposing two beams at an angle), creating alternating regions of high and low absorption on which the resonant probe beam can diffract [8,9]. A phase EIG typically involves a four-level atom, where a weak coupling to the fourth level disturbs the EIT condition by mainly altering the atomic dispersion while maintaining a low probe absorption. Modulation of the additional coupling channel, via a third excitation laser [10,11] or a microwave field [12], leads to a spatially varying index of refraction. A phase grating can also be induced in a three-level atom in the limit of a very strong coupling field [6]. Common to all of these EIG schemes is the fact that they are wavelength specific. They can only diffract a probe beam tuned to the particular atomic transition linked to the EIT coupling field.

We here propose an EIG that can diffract a probe wave resonantly tuned to any excited atomic state accessible by a dipole transition from the atom's ground state. This EIG is implemented in an atomic system in a double-Λ, nondegenerate configuration with one of the upper excited states chosen freely. Two copropagating driving fields are Raman resonant and pump the atoms into a maximally coherent dark state, forming a coherence grating in the ground states of the Raman transition along the propagation direction. The enhanced nonlinearity of the EIT medium allows an efficient four-wave mixing (FWM) that originates from the diffraction of the probe field off the coherence grating. We show that modulation of the driving fields in a direction perpendicular to propagation generates an EIG that further diffracts simultaneously the probe and the FWM fields.

FWM processes in the context of EIT or CPT involving a double-Λ scheme have been studied previously [13–18]. For completeness, in Sec. II we review the basic features of FWM under maximal atomic coherence in the double-Λ atom. We discuss our proposal for an EIG under maximal coherence in Sec. III, and we conclude the paper in Sec. IV.

II. MODEL ATOMIC SYSTEM FOR MAXIMAL-COHERENCE, FOUR-WAVE MIXING

The atomic model consists of a closed, four-level double-Λ system interacting with three cw lasers as shown in Fig. 1(a). Levels $|a\rangle$ and $|d\rangle$ are excited states that decay spontaneously at rate γ to both lower levels. Level $|c\rangle$ is the ground state, and $|b\rangle$ is a metastable state with negligible decay rate ($\gamma_0 \ll \gamma$). The $|a\rangle \rightarrow |b\rangle$ and $|a\rangle \rightarrow |c\rangle$ transitions are excited by resonant driving beams B and C, respectively. The probe beam P couples the ground state $|c\rangle$ to the excited state $|d\rangle$. The $|d\rangle \rightarrow |b\rangle$ transition is driven by field S, which is generated through FWM. Fields B and C are strong while P and S are weak. The driving fields B and C optically pump the atom into a dark superposition state of the lower levels. Under CPT, the atom becomes decoupled from the B and C fields. In an extended atomic sample, those two fields will propagate as if in free space without losses [1,7] whenever their linewidth is smaller than the homogeneous linewidth γ of the atoms. Inside the atomic sample, the four beams are collinear and propagate along the z direction, as illustrated in Fig. 1(b). We assume a homogeneously broadened medium.

The electric field of the excitation beams is defined as

$$E(\omega_j,t) = E_j \exp(i\omega_j t - ik_j z), \tag{1}$$

where $j = b,c,p,s$; ω_j is the optical frequency of field j; and k_j is its wave number. The coupling between the atom and the electric fields is defined by the Rabi frequency $\Omega_j \exp(-ik_j z)$, where $\Omega_j = 2\mu_{nm}E_j/\hbar$, and μ_{nm} is the electric dipole moment of the respective transition.

*araujo@ifi.unicamp.br

In the rotating-wave approximation, the equations of motion for the density matrix elements of levels $|a\rangle$, $|b\rangle$, $|c\rangle$, and $|d\rangle$ are

$$\begin{aligned}
\dot{\sigma}_{aa} &= -\gamma\sigma_{aa} + \frac{i}{2}(\Omega_b^*\sigma_{ab} - \Omega_b\sigma_{ba}) + \frac{i}{2}(\Omega_c^*\sigma_{ac} - \Omega_c\sigma_{ca}),\\
\dot{\sigma}_{ab} &= -\frac{\gamma}{2}\sigma_{ab} + \frac{i}{2}\Omega_b(\sigma_{aa} - \sigma_{bb}) - \frac{i}{2}\Omega_c\sigma_{cb} + \frac{i}{2}\Omega_s\sigma_{ad},\\
\dot{\sigma}_{ac} &= -\frac{\gamma}{2}\sigma_{ac} - \frac{i}{2}\Omega_b\sigma_{bc} + \frac{i}{2}\Omega_c(\sigma_{aa} - \sigma_{cc}) + \frac{i}{2}\Omega_p\sigma_{ad},\\
\dot{\sigma}_{ad} &= -\gamma\sigma_{ad} - \frac{i}{2}\Omega_b\sigma_{bd} - \frac{i}{2}\Omega_c\sigma_{cd} + \frac{i}{2}\Omega_p^*\sigma_{ac} + \frac{i}{2}\Omega_s^*\sigma_{ab},\\
\dot{\sigma}_{bb} &= \frac{\gamma}{2}\sigma_{aa} - \gamma_0\sigma_{bb} + \gamma_0\sigma_{cc} + \frac{\gamma}{2}\sigma_{dd} - \frac{i}{2}(\Omega_b^*\sigma_{ab} - \Omega_b\sigma_{ba})\\
&\quad + \frac{i}{2}(\Omega_s\sigma_{bd} - \Omega_s^*\sigma_{db}),\\
\dot{\sigma}_{bc} &= -\gamma_0\sigma_{bc} - \frac{i}{2}\Omega_b^*\sigma_{ac} + \frac{i}{2}\Omega_c\sigma_{ba} + \frac{i}{2}\Omega_p\sigma_{bd} - \frac{i}{2}\Omega_s^*\sigma_{dc},\\
\dot{\sigma}_{cc} &= \frac{\gamma}{2}\sigma_{aa} + \gamma_0\sigma_{bb} - \gamma_0\sigma_{cc} + \frac{\gamma}{2}\sigma_{dd} + \frac{i}{2}(\Omega_c\sigma_{ca} - \Omega_c^*\sigma_{ac})\\
&\quad + \frac{i}{2}(\Omega_p\sigma_{cd} - \Omega_p^*\sigma_{dc}),\\
\dot{\sigma}_{db} &= -\frac{\gamma}{2}\sigma_{db} + \frac{i}{2}\Omega_b\sigma_{da} - \frac{i}{2}\Omega_p\sigma_{cb} + \frac{i}{2}\Omega_s(\sigma_{dd} - \sigma_{bb}),\\
\dot{\sigma}_{dc} &= -\frac{\gamma}{2}\sigma_{dc} + \frac{i}{2}\Omega_c\sigma_{da} - \frac{i}{2}\Omega_s\sigma_{bc} + \frac{i}{2}\Omega_p(\sigma_{dd} - \sigma_{cc}),\\
\dot{\sigma}_{dd} &= -\gamma\sigma_{dd} + \frac{i}{2}(\Omega_p^*\sigma_{dc} - \Omega_p\sigma_{cd}) + \frac{i}{2}(\Omega_s^*\sigma_{db} - \Omega_s\sigma_{bd}).
\end{aligned} \tag{2}$$

Equations (2) are solved in the steady-state regime. To zero order in the probe and signal fields, the Raman coherence between the lower levels is

$$\sigma_{bc}^{(0)} = -\frac{\Omega_b^*\Omega_c}{|\Omega_b|^2 + |\Omega_c|^2 + 2\gamma\gamma_0}\exp[i(k_b - k_c)z]. \tag{3}$$

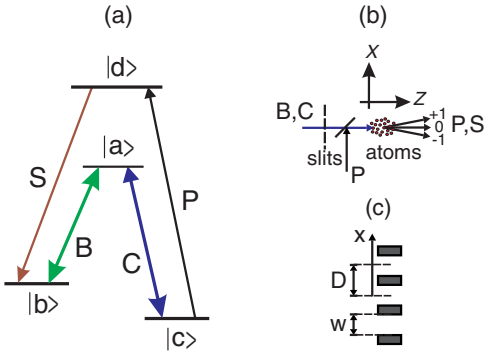

FIG. 1. (Color online) (a) Energy-level diagram of the four-level, double-Λ system driven by three optical fields: driving (B and C) and probe (P) beams in a four-wave mixing configuration giving rise to the signal beam (S). (b) Illustration of the proposed setup for an EIG with maximal coherence. Multiple slits are added to the B and C fields which are combined in a beam splitter with the probe field in a collinear configuration. The z axis is parallel to the propagation direction. The probe and signal fields diffract along the transverse x direction. (c) Intensity mask to be added to the driving fields consisting of multiple slits of width w separated by D.

No approximations were made with respect to the Rabi frequencies Ω_b and Ω_c in deriving Eq. (3). In the limit $|\Omega_b|^2 + |\Omega_c|^2 \gg 2\gamma\gamma_0$, the Raman coherence is $|\sigma_{bc}^{(0)}| = 1/2$. And for equal Rabi frequencies $\Omega_b = \Omega_c = \Omega$, the populations in the lower states are equal ($\sigma_{bb}^{(0)} = \sigma_{cc}^{(0)} = 1/2$), placing the atom in a condition of maximal coherence of the Raman transition $|b\rangle \to |c\rangle$. CPT writes a sinusoidal grating in the phase of the ground-state coherence $\sigma_{bc}^{(0)}$ along the z direction. Diffraction of the probe beam P on this grating generates the signal beam S [13].

To first order in the probe and signal fields, we find the atomic coherences of the $|d\rangle \to |b\rangle$ and $|d\rangle \to |c\rangle$ transitions to be given by

$$\begin{aligned}
\sigma_{bd}^{(1)} &= i[-r\,\Omega_p^*\,e^{i(k_p + k_b - k_c)z} + s\,\Omega_s^*\,e^{ik_s z}],\\
\sigma_{cd}^{(1)} &= i[s\,\Omega_p^*\,e^{ik_p z} - r\,\Omega_s^*\,e^{i(k_s - k_b + k_c)z}],
\end{aligned} \tag{4}$$

where the coefficients r and s are

$$\begin{aligned}
r &= \frac{\Omega^2}{2\gamma(\Omega^2 + \gamma_0\gamma)},\\
s &= \frac{\Omega^4 + \gamma^2(\Omega^2 + \gamma\gamma_0)}{2\gamma(\Omega^2 + \gamma_0\gamma)(\Omega^2 + \gamma^2)}.
\end{aligned} \tag{5}$$

We are interested in two limits of excitation: $\Omega = 0$ (driving fields off) and $\Omega^2 \gg \gamma\gamma_0$ (driving fields on). In the former limit, $r = 0$, and $s = 1/2\gamma$. And in the latter, $r = s = 1/2\gamma$.

Under the slowly varying envelope approximation, propagation of the probe and signal fields is described by the reduced wave equation, expressed as

$$\frac{\partial E_{p,s}(z)}{\partial z} = i\frac{k}{2\epsilon_0}P_{p,s}e^{-ik_{p,s}z}, \tag{6}$$

with the macroscopic atomic polarization $P_{p,s}$ serving as the driving source for the fields. The atomic polarization can be obtained by taking the ensemble average of the dipole moment: $P_p = N\mu_{dc}\sigma_{dc}$ and $P_s = N\mu_{db}\sigma_{bd}$, where N is the atomic density. The field amplitudes obey the resulting set of coupled equations

$$\begin{aligned}
E_p' &= -(\alpha/2)E_p + \kappa E_s e^{i\Delta kz},\\
E_s' &= -(\alpha/2)\Lambda E_s + \kappa\Lambda E_p e^{-i\Delta kz},
\end{aligned} \tag{7}$$

where the primes indicate differentiation with respect to z; $\alpha = 2\gamma s/z_0$ is the absorption coefficient; $\kappa = \gamma r/z_0$ is the coupling constant; $\Lambda = \lambda_p/\lambda_s$ is the ratio of probe and signal wavelengths; $z_0 = \hbar\epsilon_0\lambda_p\gamma/2\pi N\mu_{dc}^2$, the probe absorption length in the absence of the driving fields ($\Omega = 0$); and $\Delta k = k_s - k_p + k_c - k_b$. Since inside the atomic sample all four beams are copropagating and resonant to their respective transitions, the required phase-matching condition $\Delta k = 0$ is satisfied. In Eqs. (7), κ couples the probe and signal fields. In the absence of the B and C driving fields ($\Omega = 0$), $\kappa = 0$ and $\alpha = 1/z_0$. For $\Omega^2 \gg \gamma\gamma_0$, $\kappa = 1/2z_0$ and $\alpha = 1/z_0$. In our analysis, we assume that the intensities of the weak probe and signal waves are low enough that changes in the strong driving fields B and C due to FWM conversion can be neglected. In this excitation limit, coherent anti-Stokes scattering, which would affect the ground-state coherence [19], can also be ignored. Although analytic solutions to Eqs. (7) are possible

for arbitrary Λ [17], we restrict our analysis to atomic systems for which $\Lambda \approx 1$, such as the D_1 line of an alkaline atom.

General solutions to Eqs. (7) are of the form

$$E_p(z) = A_0 \exp(\xi_0 z) + B_0 \exp(\xi_1 z), \tag{8}$$

$$E_s(z) = A_1 \exp(\xi_0 z) + B_1 \exp(\xi_1 z), \tag{9}$$

where $A_{0,1}$ and $B_{0,1}$ are constants. Substituting Eqs. (8) and (9) into the coupled wave equations (7), we obtain the wave numbers

$$\xi_{0,1} = -\frac{\alpha}{2} \pm \kappa = \frac{\gamma}{z_0}(-s \pm r) \tag{10}$$

with the plus sign corresponding to ξ_0 and the minus sign to ξ_1. To determine the constants $A_{0,1}$ and $B_{0,1}$, we need to specify the boundary conditions. We take the amplitude of the probe wave to be unity $[E_p(0) = 1]$ and that of the signal wave to be zero $[E_s(0) = 0]$ at $z = 0$. From these conditions, we find $A_0 = B_0 = \frac{1}{2}$ and $A_1 = -B_1 = \frac{1}{2}$, yielding

$$E_p(z) = \exp(-\alpha z/2)\cosh(\kappa z), \tag{11}$$

$$E_s(z) = \exp(-\alpha z/2)\sinh(\kappa z). \tag{12}$$

Figure 2 shows the amplitude of probe and signal waves as a function of propagation distance calculated from Eqs. (11) and (12). In the absence of the driving fields, we have $\kappa = 0$, and the probe amplitude E_p simply decays exponentially with distance z; the signal field is null. With the strong driving fields on, $\kappa \neq 0$, the probe and signal fields exchange energy during propagation. The signal field grows in amplitude until it is large enough that the two terms in the right-hand sides of Eqs. (7) cancel each other, and the probe and signal fields propagate without attenuation or amplification thereafter. Once EIT for both probe and signal fields is established, no further production of the signal field occurs in the rest of the medium. A maximum of 25% of the incident probe energy is converted into the signal light, which agrees with Ref. [18].

III. EIG WITH MAXIMAL COHERENCE

We propose that, in addition to the coherence grating, an EIG can be further induced in the atomic sample by adding an intensity mask (multiple slits, for example) to the driving B and C fields, as illustrated in Fig. 1(b). The slits create alternating regions of high and low absorption of the probe beam along the transverse x direction, mimicking an absorption grating. But they also modulate along x the FWM process that generates the signal field. Therefore, both probe and signal fields will diffract as a result of the transverse modulation.

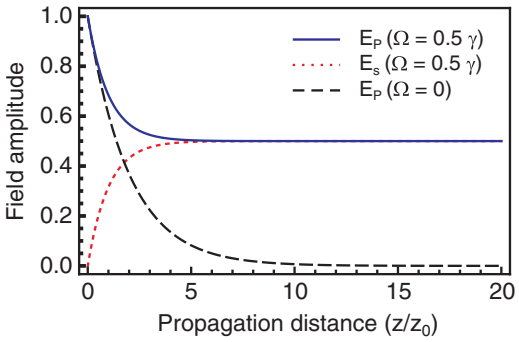

FIG. 2. (Color online) Probe and signal wave amplitudes as a function of propagation distance (in units of the probe absorption length z_0) with driving fields on ($\Omega = 0.5\gamma$) and off ($\Omega = 0$). Field amplitudes are normalized such that, at the input, the probe amplitude is $E_p(0) = 1$. We used $\gamma_0 = 0.001\gamma$.

The mask consists of a regular series of slits that simply block or let through the driving fields:

$$\Omega(x) = \Omega \sum_{m=-M/2}^{M/2} \mathrm{rect}\left(\frac{x - m\,D}{w}\right), \tag{13}$$

where $\mathrm{rect}(x)$ is the rectangle function, and M is the number of slits. Each slit has width w, with centers separated by D. This mask is illustrated in Fig. 1(c).

If we consider typical excitation parameters for the D_1 line of a ^{87}Rb atom, $\gamma = 2\pi \times 6$ MHz, $\mu_{dc} = 2.54 \times 10^{-29}$ Cm, $N = 10^{11}$ cm^{-3}, and $\lambda_p = 795$ nm, then $z_0 = 68\ \mu$m. An atomic sample of length $L = 10z_0$ will correspond to $L = 0.7$ mm. Taking $\lambda_c \approx \lambda_b \approx 795$ nm, then for a slit width of $w = 200\lambda_b \approx 160\ \mu$m, the Fresnel number associated with the B and C driving fields is $\mathcal{F} = w^2/L\lambda_{b,c} \approx 46$. Therefore, propagation of the driving fields within the atomic sample is described by geometrical optics, and the boundary of the light transmitted by the slits is sharp and resembles the slits in shape. We can neglect diffraction of these beams while inside the atomic sample and write the Rabi frequency, throughout the atomic sample, as in Eq. (13) to a good approximation. For atomic samples shorter than $L = 10z_0$, the beam Fresnel number will be even higher and the approximation will still be valid, but it may not hold for much longer samples.

With the choice of transverse modulation expressed in Eq. (13) and from Eqs. (11) and (12), we find the transmission functions of the atomic sample for the probe $[T_p(x)]$ and signal $[T_s(x)]$ fields, for one slit period ($|x| \leqslant D/2$),

$$T_p(x) = \begin{cases} (1 + \exp[-L/z_0])/2, & \text{if } |x| < w/2, \\ \exp[-L/2z_0], & \text{otherwise,} \end{cases} \tag{14}$$

and

$$T_s(x) = \begin{cases} (1 - \exp[-L/z_0])/2, & \text{if } |x| < w/2, \\ 0, & \text{otherwise.} \end{cases} \tag{15}$$

Both transmission functions are real, indicating the EIG is a pure absorption grating, with no phase modulation of the probe and signal electric-field amplitudes.

Figure 3 shows the probe and signal transmission functions for two different medium lengths: $L = 2z_0$ and $L = 10z_0$. In those regions where the driving fields are on, $T_p = T_{p,\mathrm{on}} \equiv (1 + \exp[-L/z_0])/2$ and $T_s = T_{s,\mathrm{on}} \equiv (1 - \exp[-L/z_0])/2$. For a long enough sample, such as $L = 10z_0$, $T_{p,\mathrm{on}} \approx T_{s,\mathrm{on}} \approx 0.5$. Wherever the driving fields are off, $T_s = T_{s,\mathrm{off}} \equiv 0$ since there is no FWM generation, and $T_p = T_{p,\mathrm{off}} \equiv \exp[-L/2z_0]$ because the probe field is simply absorbed as it propagates along the atomic sample. The depth of probe modulation depends on the medium thickness. For an optically thin sample, less of the probe light is absorbed in the absence of the driving fields, and the dark regions of the EIG are not opaque enough for it to efficiently diffract the probe light. In the example of Fig. 3(a), for $L = 2z_0$, the atomic medium transmits close to 38% of the probe amplitude with the driving fields off.

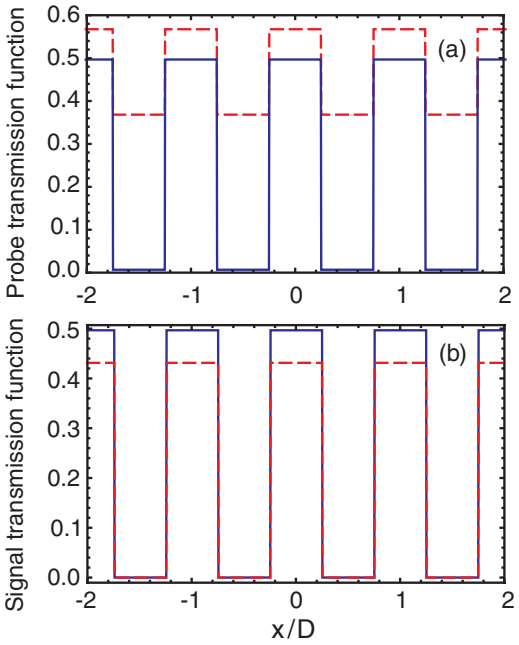

FIG. 3. (Color online) (a) Probe and (b) signal transmission functions plotted vs the transverse distance x (in units of the grating period D) for $L = 2z_0$ [dashed (red) line] and $L = 10z_0$ [(solid (blue) line]. In regions of high transmission, the driving fields are on, and in regions of low transmission, the fields are off. The slit width was chosen to be $w = D/2$.

For full modulation of the probe wave, a thickness L such that $T_{p,\text{off}} \ll 1$ is required. For $L = 10z_0$, less than 1% of the probe amplitude is transmitted. A much thicker sample maybe not be of interest since it may lead to diffraction of the driving fields inside the sample, as discussed in the paragraph following Eq. (13). In contrast, the signal field always experiences full modulation of its amplitude, although for too thin a medium, its peak amplitude may be too small. A small decrease in transmission amplitude between the $L = 2z_0$ and $L = 10z_0$ cases is seen in Fig. 3(b).

If the atomic sample is normally illuminated by the probe wave, the probe and signal amplitude distribution in the far field is

$$U_{p,s}(\theta) = \mathcal{C}\int_{-\infty}^{\infty} T_{p,s}(x)\exp(-2\pi i Dx\sin\theta/\lambda)\,dx, \qquad (16)$$

where θ is the diffraction angle, $\mathcal{C}$ is a proportionality constant, and $\lambda = \lambda_p \approx \lambda_s$. Substituting Eqs. (14) and (15) into Eq. (16), we find the diffracted probe amplitude

$$\begin{aligned} U_p(\theta) = {} & (\mathcal{C}MD)\{(w/D)T_{p,\text{on}}\text{sinc}[(\pi w/\lambda)\sin\theta] + (a/D)T_{p,\text{off}} \\ & \times \exp[-i(\pi D/\lambda)\sin\theta]\,\text{sinc}[(\pi a/\lambda)\sin\theta]\} \\ & \times \frac{\sin[M(\pi D/\lambda)\sin\theta]}{M\sin[(\pi D/\lambda)\sin\theta]} \end{aligned} \qquad (17)$$

and the diffracted signal amplitude

$$\begin{aligned} U_s(\theta) = {} & (\mathcal{C}MD)(w/D)T_{s,\text{on}}\,\text{sinc}[(\pi w/\lambda)\sin\theta] \\ & \times \frac{\sin[M(\pi D/\lambda)\sin\theta]}{M\sin[(\pi D/\lambda)\sin\theta]}, \end{aligned} \qquad (18)$$

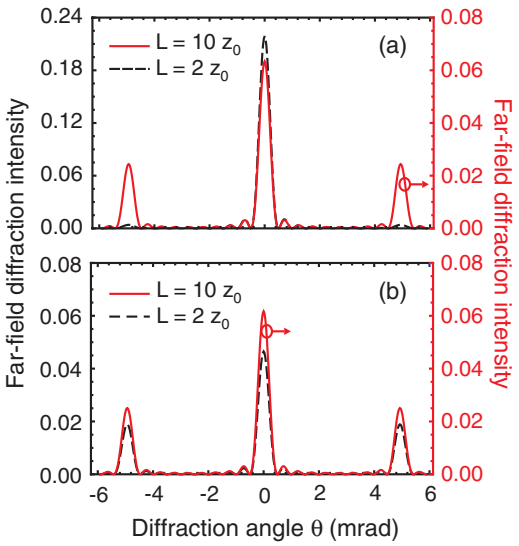

FIG. 4. (Color online) Fraunhoffer diffraction patterns for the (a) probe and (b) signal waves. The intensity is normalized such that if $T_p(x) = 1$, then $I_p(\theta = 0) = 1$.

where $a = D - w$ is the width of the (partially) opaque region between slits, and $M = 10$. The second term inside the curly braces in the right-hand side of Eq. (17) plays a role only if the grating slits are partially opaque. For fully opaque slits, $T_{p,\text{off}} \approx 0$. From Eqs. (17) and (18), the diffraction intensity distribution $I_{p,s}(\theta) = |U_{p,s}(\theta)|^2/(\mathcal{C}MD)^2$ can be calculated. The diffraction intensity is normalized such that if $T_p(x) = 1$, for example for $L \ll 1$, then $I_p(0) = 1$.

Figure 4 illustrates the far-field diffraction patterns for probe and signal fields calculated based on the transmission functions of Fig. 3. The first diffraction orders are located at $\theta \approx \pm\lambda/D = \pm 5$ mrad. In Fig. 4(a), we see that the better modulation of the probe transmission function for $L = 10z_0$ compared to $L = 2z_0$ leads to significantly more light diffracted into the first order in the former case than in the latter. For $L = 2z_0$, we get less than 0.5% of the probe light diffracted into the first order, as opposed to 2.5% for $L = 10z_0$. Since the signal transmission function is not significantly different between the two sample lengths, diffraction of the signal field into the first order is similar in the two cases, as shown in Fig. 4(b).

We can obtain an analytical expression for the probe and signal efficiencies for diffraction into the first order. Given the normalization of the diffracted intensity $I_{p,s}(\theta)$, the diffraction efficiency of the EIG into the first order for probe and signal waves is simply $I_{p,s}(\theta)$ evaluated at $\sin\theta = \lambda/D$. For fully opaque slits,

$$\eta_p = [T_{p,\text{on}}(w/D)\,\text{sinc}(\pi w/D)]^2 \qquad (19)$$

and

$$\eta_s = [T_{s,\text{on}}(w/D)\,\text{sinc}(\pi w/D)]^2. \qquad (20)$$

It is straightforward to show that $\eta_{p,s}$ reach a maximum for $w/D = 0.5$. The condition for fully opaque slits corresponds to $T_{p,\text{on}} \approx T_{s,\text{on}} \approx 0.5$ as well. Under these conditions, we calculate from Eqs. (19) and (20) a maximum probe and signal diffraction efficiency of $\eta_{p,s} \approx 2.5\%$. This value is, however,

the overall efficiency of the combined coherence grating and EIG. Because of the coherence grating, only $T_{p,\mathrm{on}}^2 \approx 25\%$ of the incident probe beam is available for diffraction from the EIG, which diverts $[(w/D)\mathrm{sinc}(\pi \mathrm{w/D})]^2 \approx 10\%$ of this light to the first order. Therefore, the diffraction efficiency of the EIG alone is higher than that of a pure-absorption sinusoidal EIG and comparable to that of the same sinusoidal EIG with phase modulation [8].

IV. CONCLUSIONS

We proposed an atomic grating that combines an absorption EIG with a coherence grating under maximal ground-state coherence. While the coherence grating diffracts a resonant probe beam into a signal beam in a traditional four-wave mixing configuration, the EIG modulates the transmission of both probe and signal beam. As a result, both beams are diffracted into ± 1 diffraction orders. An analytical expression for the diffraction efficiency was found that predicted a maximum first-order efficiency for both beams of approximately 10% for the EIG alone and 2.5% for the combined EIG and coherence grating. This analytical solution was obtained in the limit that diffraction of the driving fields within the atomic sample could be neglected. This approximation is valid if the mask that modulates the driving fields and creates the EIG consists of wide slits ($\approx$160 μm width), and the atomic sample is short ($\lesssim$1 mm).

To the best of our knowledge, all the EIGs previously described in the literature so far can diffract only the specific wavelength associated with the EIT probe transition. In contrast, our EIG simultaneously diffracts two different wavelengths (probe and signal). A significant feature of our maximal-coherence EIG is that it will work with a probe beam resonantly tuned to any dipole-allowed transition starting from the ground state. Although we illustrated our analysis for the particular case of the D_1 line of the Rb atom, the excited state to which the probe laser is connected is not limited to one of the hyperfine states of the $P_{1/2}$ atomic level. The CPT-inducing driving fields could be operating in the D_1 line while the probe field is tuned to an excited state in the D_2 line, for example. In future work, we plan to extend our model to a "multi"-Λ system consisting of a multitude of excited states. In this system, we are going to investigate the possibility of inducing a grating that will diffract probe fields simultaneously tuned to several resonant transitions, thus behaving as a wavelength demultiplexer.

ACKNOWLEDGMENT

The authors acknowledge the financial support of INOF-CNPq and FAPESP.

[1] M. Fleischhauer, A. Imamoglu, and J. P. Marangos, Rev. Mod. Phys. **77**, 633 (2005).
[2] A. W. Brown and M. Xiao, Opt. Lett. **30**, 699 (2005).
[3] S.-q. Kuang, R.-g. Wan, J. Kou, Y. Jiang, and J.-y. Gao, J. Opt. Soc. Am. B **27**, 1518 (2010).
[4] M. Bajcsy, A. S. Zibrov, and M. D. Lukin, Nature (London) **426**, 638 (2003).
[5] D. Moretti, D. Felinto, J. W. R. Tabosa, and A. Lezama, J. Phys. B **43**, 115502 (2010).
[6] L. Zhao, W. Duan, and S. F. Yelin, Phys. Rev. A **82**, 013809 (2010).
[7] E. Arimondo, Prog. Opt. **35**, 257 (1996).
[8] H. Y. Ling, Y.-Q. Li, and M. Xiao, Phys. Rev. A **57**, 1338 (1998).
[9] M. Mitsunaga and N. Imoto, Phys. Rev. A **59**, 4773 (1999).
[10] L. E. E. de Araujo, Opt. Lett. **35**, 977 (2010).
[11] S. A. Carvalho and L. E. E. de Araujo, Opt. Express **19**, 1936 (2011).
[12] Z.-H. Xiao, S. G. Shin, and K. Kim, J. Phys. B **43**, 161004 (2010).
[13] P. R. Hemmer, D. P. Katz, J. Donoghue, M. Cronin-Golomb, M. S. Shahriar, and P. Kumar, Opt. Lett. **20**, 982 (1995).
[14] M. Jain, H. Xia, G. Y. Yin, A. J. Merriam, and S. E. Harris, Phys. Rev. Lett. **77**, 4326 (1996).
[15] B. Lu, W. H. Burkett, and M. Xiao, Opt. Lett. **23**, 804 (1998).
[16] A. J. Merriam, S. J. Sharpe, M. Shverdin, D. Manuszak, G. Y. Yin, and S. E. Harris, Phys. Rev. Lett. **84**, 5308 (2000).
[17] H. Kang, G. Hernandez, J. Zhang, and Y. Zhu, J. Opt. Soc. Am. B **23**, 718 (2006).
[18] M. G. Payne and L. Deng, Phys. Rev. A **65**, 063806 (2002).
[19] V. Wong, R. S. Bennink, A. M. Marino, R. W. Boyd, C. R. Stroud, Jr., and F. A. Narducci, Phys. Rev. A **70**, 053811 (2004).